

University of Wollongong

Research Online

Faculty of Engineering and Information
Sciences - Papers: Part A

Faculty of Engineering and Information
Sciences

1-1-2015

A novel approach to postmastectomy radiation therapy using scanned proton beams

Nicolas Depauw

University of Wollongong, nd999@uowmail.edu.au

Estelle Batin

Massachusetts General Hospital

Julianne Daartz

Massachusetts General Hospital

Anatoly Rosenfeld

University of Wollongong, anatoly@uow.edu.au

Judith Adams

Massachusetts General Hospital

See next page for additional authors

Follow this and additional works at: <https://ro.uow.edu.au/eispapers>



Part of the [Engineering Commons](#), and the [Science and Technology Studies Commons](#)

Recommended Citation

Depauw, Nicolas; Batin, Estelle; Daartz, Julianne; Rosenfeld, Anatoly; Adams, Judith; Kooy, Hanne; MacDonald, Shannon; and Lu, Hsiao-Ming, "A novel approach to postmastectomy radiation therapy using scanned proton beams" (2015). *Faculty of Engineering and Information Sciences - Papers: Part A*. 4222. <https://ro.uow.edu.au/eispapers/4222>

Research Online is the open access institutional repository for the University of Wollongong. For further information contact the UOW Library: research-pubs@uow.edu.au

A novel approach to postmastectomy radiation therapy using scanned proton beams

Abstract

Purpose: Postmastectomy radiation therapy (PMRT), currently offered at Massachusetts General Hospital, uses proton pencil beam scanning (PBS) with intensity modulation, achieving complete target coverage of the chest wall and all nodal regions and reduced dose to the cardiac structures. This work presents the current methodology for such treatment and the ongoing effort for its improvements. **Methods and Materials:** A single PBS field is optimized to ensure appropriate target coverage and heart/lung sparing, using an in-house-developed proton planning system with the capability of multicriteria optimization. The dose to the chest wall skin is controlled as a separate objective in the optimization. Surface imaging is used for setup because it is a suitable surrogate for superficial target volumes. In order to minimize the effect of beam range uncertainties, the relative proton stopping power ratio of the material in breast implants was determined through separate measurements. Phantom measurements were also made to validate the accuracy of skin dose calculation in the treatment planning system. Additionally, the treatment planning robustness was evaluated relative to setup perturbations and patient breathing motion. **Results:** PBS PMRT planning resulted in appropriate target coverage and organ sparing, comparable to treatments by passive scattering (PS) beams but much improved in nodal coverage and cardiac sparing compared to conventional treatments by photon/electron beams. The overall treatment time was much shorter than PS and also shorter than conventional photon/electron treatment. The accuracy of the skin dose calculation by the planning system was within $\pm 2\%$. The treatment was shown to be adequately robust relative to both setup uncertainties and patient breathing motion, resulting in clinically satisfying dose distributions. **Conclusions:** More than 25 PMRT patients have been successfully treated at Massachusetts General Hospital by using single-PBS fields. The methodology and robustness of both the setup and the treatment have been discussed.

Disciplines

Engineering | Science and Technology Studies

Publication Details

Depauw, N., Batin, E., Daartz, J., Rosenfeld, A., Adams, J., Kooy, H., Macdonald, S. & Lu, H. (2015). A novel approach to postmastectomy radiation therapy using scanned proton beams. *International Journal of Radiation Oncology Biology Physics*, 91 (2), 427-434. *International Journal of Radiation: Oncology Biology Physics*

Authors

Nicolas Depauw, Estelle Batin, Julianne Daartz, Anatoly Rosenfeld, Judith Adams, Hanne Kooy, Shannon MacDonald, and Hsiao-Ming Lu

A novel approach to post-mastectomy radiation therapy using scanned proton beams.

Nicolas Depauw MS^{1,2}, Estelle Batin PhD¹, Julianne Daartz PhD¹,
Anatoly Rosenfeld PhD², Judith Adams¹, Hanne Kooy PhD¹, Shannon MacDonald MD¹, Hsiao-
Ming Lu PhD¹

¹Francis H. Burr Proton Therapy Center, Department of Radiation Oncology,
Massachusetts General Hospital (MGH), Boston MA 02114, USA

²Centre for Medical Radiation Physics, University of Wollongong,
Northfields Avenue, NSW 2522, Australia

Running title: Post-mastectomy radiation therapy using IMPT.

Corresponding Author:

Nicolas Depauw

55 fruit Street,

Boston, MA 02114

617-643-6970 (W)

617-646-9566 (C)

ndepauw@partners.org

Conflict of interest: None.

A novel approach to post-mastectomy radiation therapy using scanned proton beams

Running title: Post-mastectomy radiation therapy using IMPT

Abstract

Purpose: Post-mastectomy radiation therapy (PMRT) is currently offered at *the institution* using proton pencil beam scanning (PBS) with intensity modulation, achieving complete target coverage of chest wall and all nodal regions and reduced dose to the cardiac structures. This work presents the current methodology in place for such treatment, and the on-going effort for its improvements.

Materials and methods: A single PBS field is optimized to ensure appropriate target coverage and heart/lung sparing, using an in-house developed proton planning system with the capability of multi-criteria optimization (MCO). The dose to chest wall skin is controlled as a separate objective in the optimization. Surface imaging is used for setup as it is a suitable surrogate for superficial target volumes. In order to minimize the effect of beam range uncertainties, the relative proton stopping power ratio (RSP) of the material in breast implants was determined through separate measurements. Phantom measurements were also performed to validate the accuracy of skin dose

calculation in the treatment planning system. Additionally, the treatment planning robustness was evaluated against setup perturbations and patient breathing motion.

Results: PBS PMRT planning results in appropriate target coverage as well as organ sparing, comparable to treatments by passive scattering (PS) beams, but much improved in nodal coverage and cardiac sparing compared to conventional treatments by photon/electron beams. The overall treatment time is much shorter than PS, and also shorter than conventional photon/electron treatment. The accuracy of the skin dose calculation by the planning system is within ± 2 %. The treatment was shown to be adequately robust against both setup uncertainties and patient breathing motion, resulting in clinically satisfying dose distributions.

Conclusions: Over 25 PMRT patients have been successfully treated at *the institution* using single PBS fields. The methodology and robustness of both the setup and the treatment were demonstrated.

1 Introduction

Radiation therapy has been an effective tool in the management of breast cancer [1]. There are, however, concerns of late cardiac effects due to this treatment [2-8]. Minimizing the dose to the heart has been the focus of various treatment improvements including the use of heart blocks, CT-based planning, intensity modulation, etc. [9]. Breath holding is one of the most effective techniques in

reducing the volume of cardiac tissues for **conventional photon therapy using tangent fields** and is currently practiced in many institutions [10, 11], even though its efficacy has recently been questioned [12].

Despite these efforts, target volumes cannot be fully covered while avoiding the cardiac tissues for many patients. This is true for post-mastectomy radiation therapy (PMRT) with involved internal mammary nodes (IMN) for patients with unfavorable cardiac anatomy. The standard PMRT treatment technique uses a combination of photon/electron beams with up to five fields involving multiple field matching. The optimization of such complex plans usually takes tremendous efforts in order to balance between IMN coverage, heart dose, hot and cold spots. The distinctive physical properties of the proton beam, i.e. the Bragg peak, offers new possibilities in meeting the challenges of PMRT. Several treatment planning studies have demonstrated significant dosimetric advantages for reducing heart and lung doses while improving target coverage [13-17]. Thus, a proton PMRT clinical trial was started at *the institution* and early outcomes showed that the treatment was well tolerated [18].

A first set of patients was treated with en face passively scattered (PS) proton beams. While the treatments achieved the primary goals of minimizing the dose to the heart and lungs, and adequately covering the chest wall and involved nodes, several aspects of the treatment were less than ideal. The largest effective field size ($\pm 2\%$ dose

homogeneity) for a PS beam is 22 cm in diameter. Most patients therefore required abutting fields, one for chest wall/IMN and one for the superior nodal targets. The matchline between the two fields had to be feathered, requiring two sets of hardware (aperture and compensators). The overall treatment generally took ≥ 30 minutes. Moreover, the lack of intensity modulation resulted in full skin dose and dose heterogeneities.

Proton pencil beam scanning (PBS) is gradually becoming available in proton therapy centers worldwide. Two of the most distinctive features of PBS, intensity modulation and larger treatment field size, are critical elements for improving proton PMRT. This work describes *the institution* PBS PMRT treatment technique, its validation, as well as the ongoing efforts performed to ameliorate its delivery.

2 Materials and methods

2.1 Patient setup and CT scanning

The PMRT patients were positioned on a breast board used for conventional photon/electron treatment with both arms up above their head. The breast board angle was raised to its limit to help with the surface imaging system used for patient setup. Various improvements were deployed in order to minimize setup position errors: a head & neck head cup was used to better control the neck position; hand grips and a chin strap were provided to further immobilize the arm and chin positions. Figure 1(a) shows the setup at *the institution* with the patient's arms raised above their head.

Figure 1(b) also shows the same patient in a arm down position. For some patients, this akimbo position was the only choice for radiotherapy due to some immobility factors. As later discussed, this position presents convenient aspects. A helical CT scan of the patient at quiet respiration was acquired using a *GE Medical Systems*TM *LightSpeed RT16* or *Discovery CTR590 RT* at 140 kV and ≈ 500 mA with 2.5 mm slice thickness.

2.2 Treatment planning

Similar delineation of the target volumes and organs at risk (OAR) are performed for PBS treatment as for conventional photon therapy. The target (CTV) is usually composed of the whole chest wall and lymph nodes considered at risk for harboring disease (axillary, supraclavicular, internal mammary).

Planning objectives are generally defined as follow:

- 45 Gy(RBE) to the chest wall and all nodes followed by a 5.4 Gy(RBE) boost to the chest wall and internal mammary nodes (IMN)
- 48 Gy(RBE) max dose to the chest wall's skin (≈ 3 mm superficial)
- 3 Gy(RBE) max dose to the left anterior descending coronary artery (LAD)
- 5 Gy(RBE) max dose to the heart's left ventricle
- ≤ 1 Gy(RBE) mean heart dose
- $\leq 15\%$ V_{20} for each lung
- 42 Gy(RBE) max dose to the thyroid

- 40 Gy(RBE) max dose to the esophagus

RBE (relative biological effectiveness) corresponds to the ratio of x- or γ -ray absorbed dose (Gy) to that of a modality (Gy(RBE)) to obtain the same biological end point. A RBE value of 1.1 is considered for protons [19].

TPS-name, an in-house treatment planning software (TPS) with multi-criteria optimization (MCO) was used. PMRT plans used a PBS field at a given gantry angle (30° from vertical). Beam spots were placed on a fixed-size grid, extending 15 mm around the assigned target volume, with spots spaced at one sigma (spot size). In depth, scanning layers were spaced by $0.8 \times$ the distal 80 % Bragg peak width. Due to machine limitations, an 8 cm range shifter was used to appropriately reach the superficial targets. *the institution's* clinical machine presents a 9 to 16 mm spot size as a function of energy. Pareto-optimal plans were generated to meet the given constraints [20]. Finally, the set of Pareto-optimal plans were navigated to a desired state.

2.3 Beam range uncertainty

Beam range uncertainty due to inaccurate CT HU to proton stopping power conversion is always a concern and the usual practice at the institution is to add an extra 3.5 % to the beam range to head off the potential undershooting. For patients without breast implant, the chest wall target volumes are usually very shallow with the required beam range at 3 cm or less. The associated uncertainty is thus only around a

millimeter and can be practically ignored, being comparable to uncertainties in CT scanning, contouring, etc. For patients with breast implants, the deeper treatment range required to reach the chest wall could result in significantly larger range uncertainties and potentially overshoot into the lung and cardiac tissues. Phantom measurements were therefore performed in order to accurately assess the relative proton relative stopping power ratio (RSP) of the exact material used inside the breast implant. During planning, the breast implants were contoured and assigned the exact RSP value based on those phantom measurements. With the contribution from the breast implants entirely eliminated, the resultant range uncertainty contains only those from the real chest wall tissue and is thus the same as those for the chest wall only treatments. The measurement techniques of determining the RSP values for the various implants and detailed analysis of the data will be reported separately.

Another possible source of range uncertainty is the daily variations in the position of the breast implant relative to the rest of the body. However, for patient with reconstructive surgery, only those with breast implants were allowed for PBS PMRT due to the extremely limited mobility of such implants.

2.4 Skin dose

Unlike photon beams, proton beams do not have dose build ups at the skin surface. It is naturally a concern if proton PMRT could increase chest wall skin toxicity, although no such increase was observed for the first group patients treated by passive

scattering [18]. With PBS, the skin dose can be controlled as one of the objectives, as shown above, in the Pareto optimization and navigation. In order to validate the accuracy of the dose calculation at the skin surface, we performed measurements for two treatment fields generated on a solid water phantom: one mimicking a non-reconstructed chest wall treatment with 3 cm beam range, and one mimicking a treatment with breast implant with 8 cm range. The accuracy of the skin dose calculation was then assessed using a Markus parallel plate ion chamber.

2.5 Treatment delivery

the institution's routine patient quality assurance (QA) procedure for PBS treatment was followed for these PMRT plans. Each PBS field was verified in phantom measurement by an absolute point dose and 2D distributions at two different depths [21].

the institution's conventional proton setup process consists of: first, the patient is positioned based on tattoos priorly inked at the time of CT-sim; orthogonal X-rays are then taken at a specified cardinal angle, and the patient precisely placed at isocenter; finally, a beamline X-ray is performed at the treatment gantry angle to finalize the setup position and ensure correct treatment. This technique was unfortunately deemed suboptimal for PMRT patients as it considers bony anatomical features in the back of the patients, such as the spine, as a surrogate for the chest wall position [22]. This resulted in the choice of surface imaging as the primary setup tool as the target

volume is both shallow and superficial. In our process, the patient is first setup based on tattoos inked at the time of CT scan. A surface imaging system (brand), using three cameras mounted in a typical triangular pattern as for a LINAC treatment room, is then used to position the patient at isocenter. Shifts are performed using the couch with 6-degree of freedom based on the treatment planning CT as the reference image. This reference provides the ability to monitor any anatomical deformation over the course of treatment. In one exemplary case, a shift of the breast implant was detected and the need for replanning was assessed through the acquisition of a new CT scan. In order to minimize the effect of breathing motion on patient positioning, the motion tracking function of the surface imaging system was utilized and the body surface corresponding to exhale level was selected for position correction calculations. The operation tolerance limits for the setup were 2 mm in translations and 1.5° in rotations. Then, a beamline X-ray is taken at the treatment gantry angle (30° from vertical) as a final verification, primarily based on three radio-opaque makers placed around the patient's chest wall at positions selected and tattooed at the time of CT. The X-ray setup tolerance was 1.5 mm. This is in consideration of the fact the X-ray is not gated to any specific breathing level. For a typical breast patient, the chest wall moves about 3 mm in the AP/longitudinal direction at quiet respiration, which projects to a motion of 1.5 mm in the beam's eye view with gantry angle at 30° from vertical. This setup process combining surface and X-ray imaging has been extensively studied for a large number of patients. The full setup process generally

takes 10 to 15 minutes. Surface imaging results in faster and more accurate patient positioning, along with minimal imaging dose (only final beamline X-ray). The techniques and detailed analyses of the results will be reported separately. The single PBS treatment field usually contains 10 to 15 layers with ≈ 2 s layer switching time, resulting in a ≈ 2 min total beam delivery time.

2.6 Treatment robustness evaluation

The treatment robustness was evaluated against two types of treatment perturbations: breathing motion and setup uncertainties. For breathing motion, a 4D-CT scan was performed for a PMRT patient in addition to the regular planning CT scan at quiet respiration. The motion of the chest wall due to breathing was found mostly in the AP direction as expected with the maximum amplitude of 3 mm, which is typical of breast patients. The PBS fields generated on the planning CT scan for the actual treatment were transferred to the 4D CT scan with dose distributions recomputed on each of the 10 phases. Dose volume histograms (DVH) were computed for each of the 10 phases as well as for the total dose accumulated through deformable registration [23], mimicking the actual treatment based on the patient's breathing cycle. The setup uncertainties analysis was performed by recomputing the dose distributions for a nominal PMRT plan with the same PBS fields but with the introduction of geometric perturbations in the isocenter position and patient body orientation. The perturbations were as follow: ± 3 mm along each translation axis (lateral, longitudinal,

vertical), $\pm 2^\circ$ along each rotation axis (yaw, pitch, roll), and a combination of all aforementioned shifts in all 6 directions simultaneously. DVH were computed for each scenario. The magnitude of these perturbations was selected in consideration of the geometric accuracy of the surface and X-ray imaging systems, as well as their operational tolerances adopted during patient setup.

3 Results

3.1 Treatment plan quality

As a result of the multi-criteria optimization, the target coverage and dose to the cardiac structures are optimally balanced through intensity modulation. Likewise, it is possible to reduce the skin dose to an acceptable level, especially in the supraclavicular nodal region, which is located deeper in the body. A nominal PBS PMRT plan is presented in figure 2.

The dose statistics for the left-sided PBS PMRT patients treated in the first 4 months of 2014 (in total of 10) at *the institution* are presented in table 1.

3.2 Skin dose validation

Measurements were performed with a Markus parallel plate ionization chamber at 0, 1, 3, 5, and 7 mm depth, as well as in the center of the field (13 and 43 mm

respectively), for both aforementioned treatment plans. The results are presented in figure 3. Those measurements were in good agreement ($\approx 2\%$) with the TPS values.

3.3 Treatment plan robustness

The robustness analysis results against setup uncertainties are presented in figure 4 as DVH envelopes which correspond to the maximum amplitude of the perturbation associated with the specified shifts, individually or simultaneously. As later discussed, this can be considered a worst case scenario, and any combination of shifts (± 3 mm, $\pm 2^\circ$) will be contained within those DVH boundaries. The DVH of the average distribution based on all these shifts is presented as a thick dashed line. Overall, the target coverage for chest wall, supraclavicular/axilla nodal regions remains quite stable, and is therefore robust against setup uncertainties. Coverage of IMN deviates substantially more from these shifts, although the minimum dose is still ≥ 40 Gy(RBE), even in the worst case scenario. Concerning OARs, DVH distributions vary more for thyroid and esophagus than for others, but all of them are still considered clinically acceptable.

The results for robustness analysis against breathing motion are shown in figure 5. As in figure 4, the DVH envelopes correspond to the maximal deviations based on the dose recomputation for each individual breathing phase. These deviations, drastically smaller than the ones observed in the robustness analysis for setup uncertainties (figure 4), are believed to be of no clinical concern. Moreover, it is admitted that the

actual treatment would be approximately at the median of these envelopes statistically, hence remarkably close to the planned dose for the case illustrated in figure 5, as highlighted by the average dose distribution DVH based on the individual recomputations (thick dashed line).

4 Discussions

PMRT for patients with potential IMN involvement and yet unfavorable cardiac anatomy is always a challenge to perform with both acceptable/reliable target coverage and critical organ avoidance. Whereas it is necessary to consider 3 to 5 fields in photon/electron therapy, or a minimum of 2 proton PS fields, in order to appropriately cover the numerous targets, a single PBS field is sufficient. In the absence of matched fields, this highly simplifies the treatment delivery and removes the hot and cold spots by means of intensity modulation. Although the treatment offers excellent cardiac structure sparing, the IMN receives on average a mean dose of 48.75 Gy(RBE) for the 10 above mentioned patients. This represents significantly better target coverage, yet better OAR sparing, than conventional therapy [16].

For PMRT by PS, certain small areas of skin may receive the full prescription dose due to the fixed modulation width of the passive scattered beams. Early results for PS PMRT patients, however, did not show worse skin reactions than for conventional X-ray treatment; contrarily, more often superficial dry, rather than moist, squamous desquamation were observed. Predicted redness of the skin within the treatment field

was also noted [18]. With intensity modulation, PBS allows one to minimize the dose to the skin while maintaining a uniform target constraint. Given the positive experience with PS treatment, patients are expected to tolerate PBS treatments equally well, if not better. It is satisfactory to see that the planning system can accurately compute the skin dose, as confirmed by the phantom measurement. Patient specific skin dose monitoring is currently under assessment at *the institution* using thermoluminescent dosimeters [24], as well as MOSkin detectors [25].

At the institution, PBS fields for chest wall treatment take significantly longer to deliver than conventional scattered fields: about 5 minutes versus 1 minute. However, the overall treatment time, that is the patient-in-room time, using PBS is only about 15 to 18 minutes, much shorter than PS treatment. This is also generally shorter than the conventional treatment with 4 photon/electron beams, which takes about 25 minutes even without any form of imaging guidance. Optimization of the current workflow is still undergoing for combined use of surface and beamline X-ray imaging, which could further reduce the setup time.

The plan robustness analyses were performed for a single patient only. Since the beam direction and patient's setup configuration are generally similar, solely the anatomical changes would significantly affect these results. This will be characterized in a future detailed study using a larger cohort of patients. It should be noted that the magnitude of the shifts and rotations were deliberately large in order to test worst case scenarios

while, in reality, the setup uncertainties are statistically much smaller. This was highlighted by the average dose distribution DVH in the robustness analysis. It is important to point out that the plan robustness analysis presented here is closely associated with the spot sizes of our current PBS delivery system and could change for different beam spot sizes. It is generally true that PBS treatment planning quality could differ per institution. Indeed, spot size, source-to-axis distance (SAD), minimum deliverable charge, and speed/accuracy of treatment delivery are highly machine specific parameters; besides, the institution's TPS would dictate the possibilities regarding spot spacing, layer spacing, and the overall quality of the optimization (notably through the presence or absence of MCO). Major efforts are currently underway *at the institution* to reduce the beam spot sizes for all beam energies including those relevant to chest wall treatment. A theoretical plan, presenting significant improvements over the plan presented in figure 2, was produced using a 3 to 5 mm spot size. A smaller beam spot size, however, could mean a longer treatment time. It may also degrade the robustness of plan against setup uncertainties and breathing motion. The implications of the spot size changes and the proper balance between all its effects will be the subjects of future studies.

One of the most interesting potential improvements of PMRT using proton therapy is the possibility of treating the patients with their arms down during treatment as shown

in figure 1(b). Such a setup position is unachievable for conventional photon therapy which uses tangent fields that would treat through the arms. The rationale for such position is based on several promising aspects. For one, it is much more comfortable than the arm up position for patients with shoulder mobility issues due to immediacy of their surgery, scaring, and other reasons. Second, patients with arms up often feel tired and relax their arms downwards, potentially affecting treatment to the axillary nodal regions, while more comfortable arm down position will result in the patient staying still for a longer period of time. Third, the arm down position allows larger clearance between the patient and the treatment nozzle, hence reducing the risk of hazardous collision. It could also allow the use of smaller air gaps between the treatment head and the patient to help maintain the spot size and improve the overall penumbra of the dose distribution. We have recently treated a patient in the arm down position and are currently collecting data for more patients in order to systematically assess this arms down setup.

Although one can foresee interplay effects between the beam motion and the patient internal motion for such treatment, these effects are considered negligible at *the institution* based on previous work on lung treatment planning [26].

5 Conclusion

We have developed a treatment technique for PMRT using pencil beam scanning with intensity modulation. More than 25 PMRT patients have been successfully treated

at *the institution*. This treatment technique is significantly simpler than conventional techniques which use a combination of photon and electron beams, yet with improved nodal coverage and significantly less cardiac dose. Although this treatment relies on full image guidance with surface and X-ray imaging, it is faster than conventional techniques. There are on-going efforts to reach the optimal PBS PMRT treatment delivery. Future studies will focus on specific aspects of the presented methodology, as well as the short-term side-effects and clinical outcomes of such PBS PMRT treatment.

References

- [1] Ragaz J, Olivotto I, Spinelli J, et al. Locoregional radiation therapy in patients with high-risk breast cancer receiving adjuvant chemotherapy: 20-year results of the British Columbia randomized trial *J Natl Cancer Inst.* 2005;97:116-126.
- [2] Darby S. C, Ewertz M, McGale P, et al. Risk of ischemic heart disease in women after radiotherapy for breast cancer *New England Journal of Medicine.* 2013;368:987-998.
- [3] Hjrís I, Overgaard M, Christensen J. J, Overgaard J. Morbidity and mortality of ischaemic heart disease in high-risk breast-cancer patients after adjuvant postmastectomy

systemic treatment with or without radiotherapy: analysis of DBCG 82b and 82c randomised trials *The Lancet*. 1999;354:1425-1430.

[4] Nilsson G, Holmberg L, Garmo H, et al. Distribution of coronary artery stenosis after radiation for breast cancer *Journal of Clinical Oncology*. 2012;30:380-386.

[5] Gagliardi G, Constine L. S, Moiseenko V, et al. Radiation dose-volume effects in the heart *International Journal of Radiation Oncology* Biology* Physics*. 2010;76:S77-S85.

[6] Gagliardi G, Lax I, Ottolenghi A, Rutqvist L. Long-term cardiac mortality after radiotherapy of breast cancer application of the relative seriality model *The British journal of radiology*. 1996;69:839-846.

[7] Gyenes G, Gagliardi G, Lax I, Fornander T, Rutqvist L. E. Evaluation of irradiated heart volumes in stage I breast cancer patients treated with postoperative adjuvant radiotherapy. *Journal of clinical oncology*. 1997;15:1348-1353.

[8] Marks L. B, Yu X, Prosnitz R. G, et al. The incidence and functional consequences of RT-associated cardiac perfusion defects *International Journal of Radiation Oncology* Biology* Physics*. 2005;63:214-223.

[9] Krueger E. A, Fraass B. A, McShan D. L, Marsh R, Pierce L. J. Potential gains for irradiation of and regional nodes with intensity modulated radiotherapy *International Journal of Radiation Oncology* Biology*Physics*. 2003;56:1023-1037.

[10] XXX

[11] Remouchamps V. M, Vicini F. A, Sharpe M. B, Kestin L. L, Martinez A. A, Wong J. W. Significant reductions in heart and lung doses using deep inspiration breath hold with active breathing control and intensity-modulated radiation therapy for patients treated with locoregional breast irradiation International Journal of Radiation Oncology* Biology* Physics. 2003;55:392-406.

[12] Zellars R, Bravo P. E, Tryggestad E, et al. SPECT Analysis of Cardiac Perfusion Changes After Whole-Breast/ Radiation Therapy With or Without Active Breathing Coordinator: Results of a Randomized Phase 3 Trial International Journal of Radiation Oncology* Biology* Physics. 2014;88:778-785.

[13] Lomax A. J, Cella L, Weber D, Kurtz J. M, Miralbell R. Potential role of intensity-modulated photons and protons in the treatment of the breast and regional nodes International Journal of Radiation Oncology* Biology* Physics. 2003;55:785-792.

[14] Weber D, Ares C, Lomax A, Kurtz J. Radiation therapy planning with photons and protons for early and advanced breast cancer: an overview Radiat Oncol. 2006;1:22.

[15] Ares C, Khan S, Macartain A, et al. Postoperative proton radiotherapy for localized and locoregional breast cancer: potential for clinically relevant improvements? Int J Radiat Oncol Biol Phys. 2010;76:685-697.

[16] XXX

[17] Jimenez R. B, Goma C, Nyamwanda J, et al. Intensity modulated proton therapy for postmastectomy radiation of bilateral implant reconstructed breasts: A treatment planning study *Radiotherapy and Oncology*. 2013;107:213-217.

[18] *XXX*

[19] A. Wambersie, RBE, reference RBE, and clinical RBE: Applications of these concepts in hadron therapy., *Strahlenther. Onkol.*, 175, Suppl. 2, pp 39-43, (1999).

[20] Craft D. L, Halabi T. F, Shih H. A, Bortfeld T. R. Approximating convex Pareto surfaces in multiobjective radiotherapy planning *Medical physics*. 2006;33:3399-3407.

[21] *XXX*

[22] Fayad H, Pan T, Clement J. F, Visvikis D. Technical note: Correlation of respiratory motion between external patient surface and internal anatomical landmarks *Medical physics*. 2011;38:3157.

[23] MIMVista, M. I. M. Software Inc., Version 6.2.5.

[24] Zullo J. R, Kudchadker R. J, Zhu X. R, Sahoo N, Gillin M. T. LiF TLD-100 as a dosimeter in high energy proton beam therapy - can it yield accurate results? *Medical Dosimetry*. 2010;35:63-66.

[25] Kelly A, Hardcastle N, Metcalfe P, et al. Surface dosimetry for breast radiotherapy in the presence of immobilization cast material *Physics in medicine and biology*. 2011;56:1001.

[26] Dowdell S, Grassberger C, Sharp G, Paganetti H. Interplay effects in proton scanning for lung: a 4D Monte Carlo study assessing the impact of tumor and beam delivery parameters *Physics in medicine and biology*. 2013;58:4137.

Captions

Figure 1: PMRT patient setup at the time of CT scan: (a) conventional arms up setup position, (b) novel arms down setup position; in both cases, a chin strap and hand grips are used for positioning reproducibility.

Figure 2: A proton PBS PMRT plan and its associated dose-volume histograms (DVH), as intended for treatment at *the institution*.

Table 1: Dose statistics for 10 PBS PMRT patients treated at *the institution*; D_{99} and D_1 are the doses in Gy(RBE) received by 99 % and 1 % of the target/OAR volume, respectively

Figure 3: Skin dose comparison between *TPS-name* computed values and Markus parallel plate ionization chamber measurements.

Figure 4: Resulting DVH envelopes based on the setup robustness analysis (± 3 mm, ± 2 °) performed on a PMRT patient plan (solid line), and compared to the average dose distribution DVH (thick dashed line) based on the individual recomputations.

Figure 5: Breathing motion effect onto a static PMRT dose distribution. The solid lines represent the planned dose while the envelopes correspond to the maximal deviations observed from the individual dose recomputations on the 10 phases of the patient 4D scan, and the thick dashed lines is the average dose distribution DVH based on all 10 recomputations.



Figure 1: PMRT patient setup at the time of CT scan: (a) conventional arms up setup position, (b) novel arms down setup position; in both cases, a chin strap and hand grips are used for positioning reproducibility.

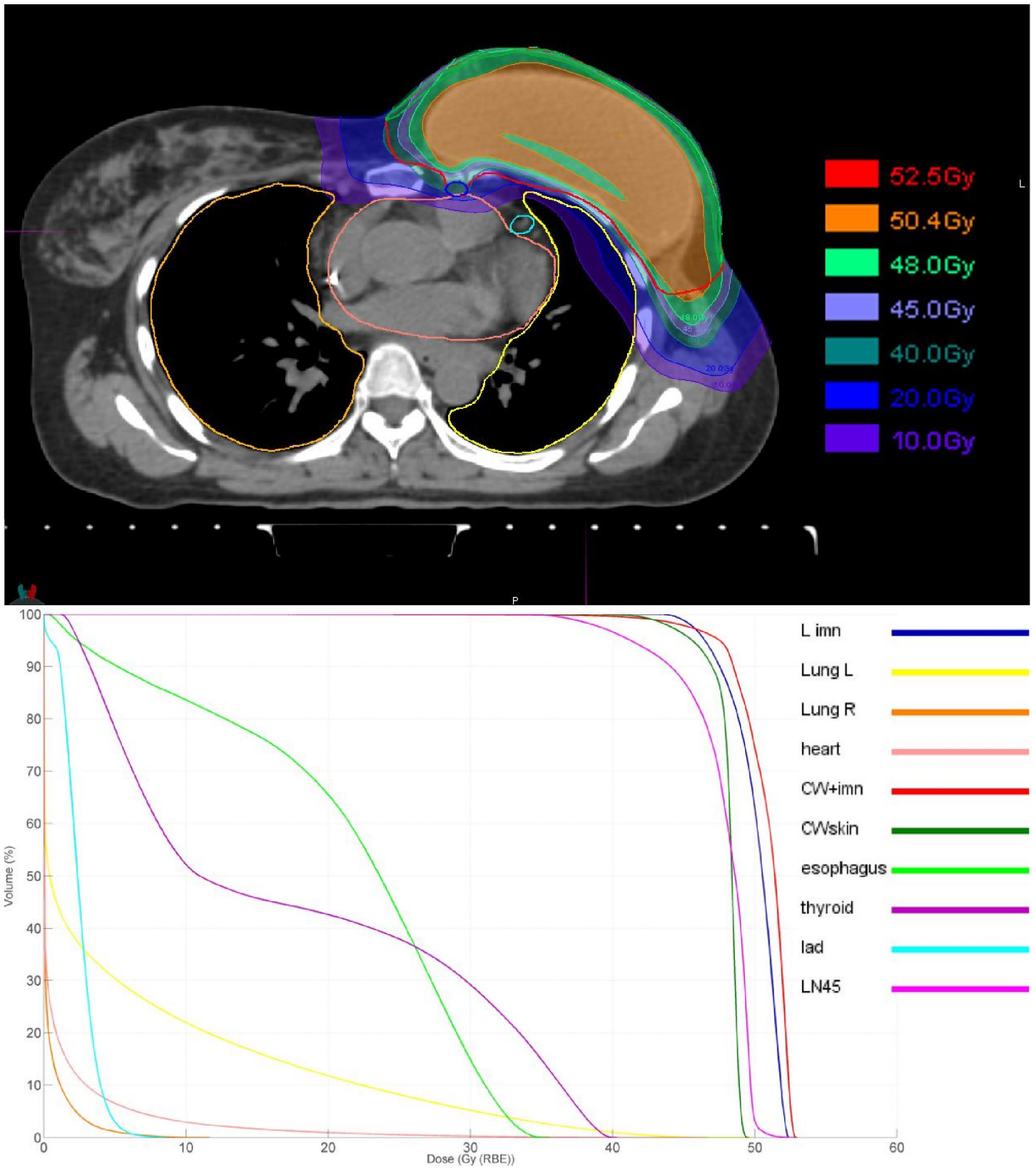


Figure 2: A proton PBS PMRT plan and its associated dose-volume histograms (DVH), as intended for treatment

at

the

institution.

Target/OAR	Mean (cGy(RBE))		D_{99} (cGy(RBE))		D_1 (cGy(RBE))	
	Average	std dev.	Average	std dev.	Average	std dev.
IMN	48.71	1.71	44.30	2.47	51.25	1.28
Lymph nodes (inc.						
IMN)	47.39	1.08	42.18	1.93	51.36	1.06
LAD	1.10	0.48	0	-	3.50	0.71
Heart	0.63	0.32	0	-	11.40	5.11
Chestwall skin	47.86	1.09	40.88	2.68	49.57	0.88

Table 1: Dose statistics for 10 PBS PMRT patients treated at *the institution*; D_{99} and D_1 are the doses in Gy(RBE) received by 99 % and 1 % of the target/OAR volume, respectively.

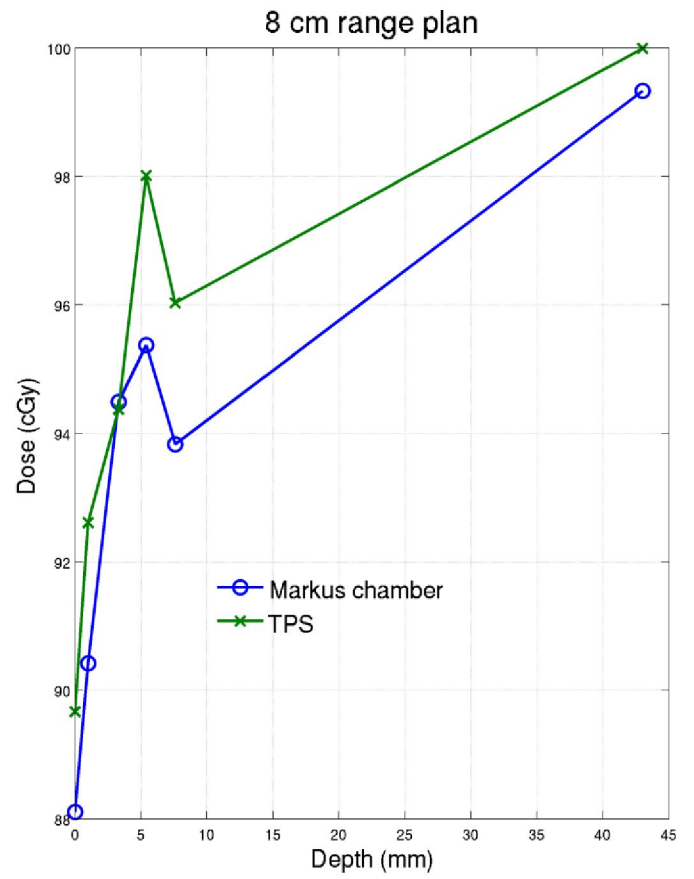
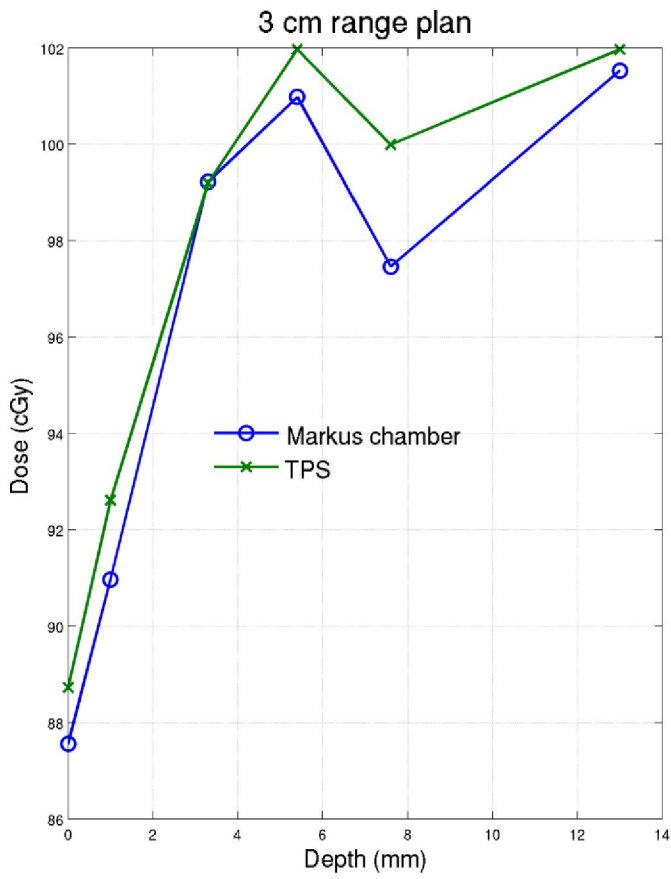


Figure 3: Skin dose comparison between TPS-name computed values and Markus parallel plate ionization chamber measurements.

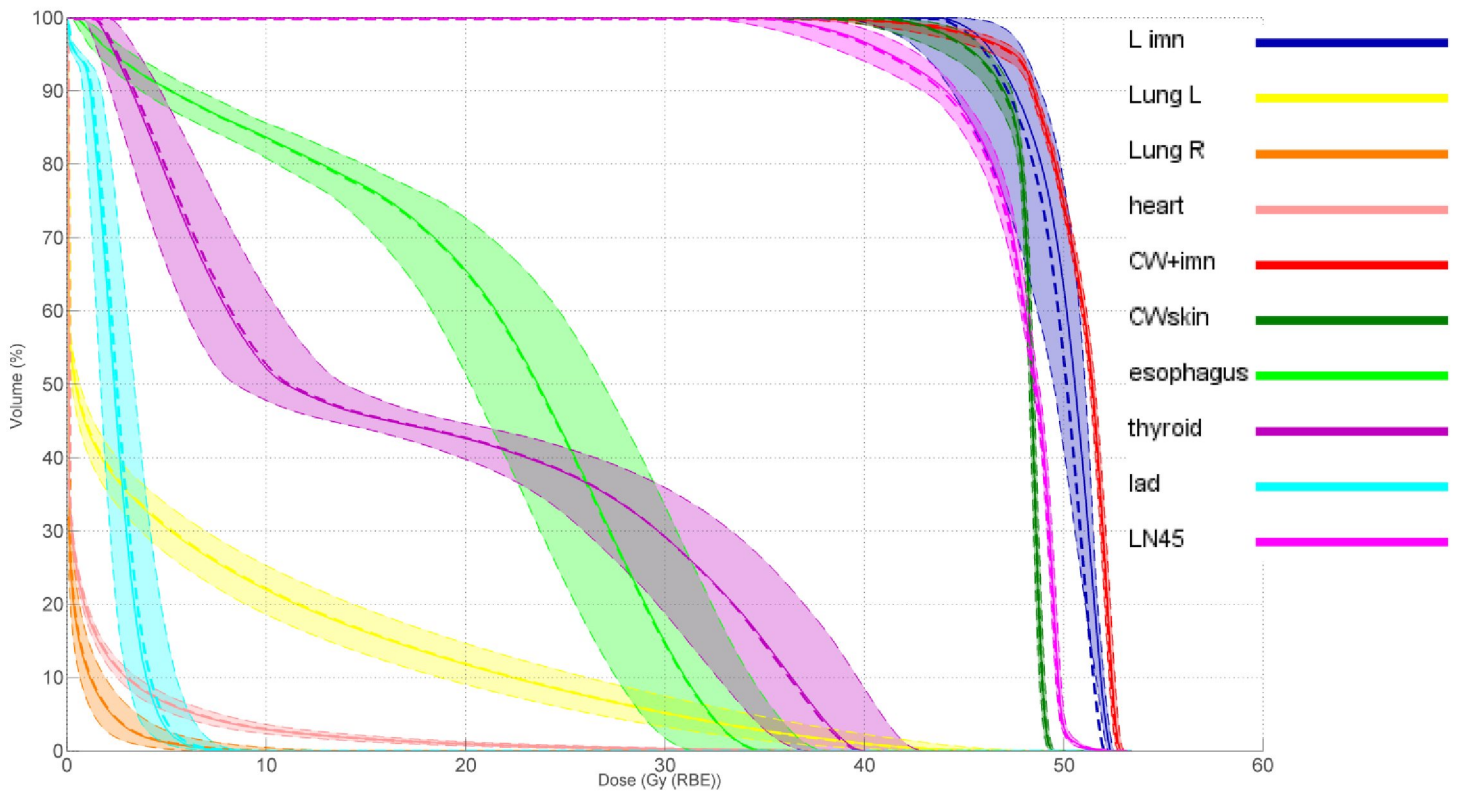


Figure 4: Resulting DVH envelopes based on the setup robustness analysis (± 3 mm, ± 2) performed on a PMRT patient plan (solid line), and compared to the average dose distribution DVH (thick dashed line) based on the individual recomputations.

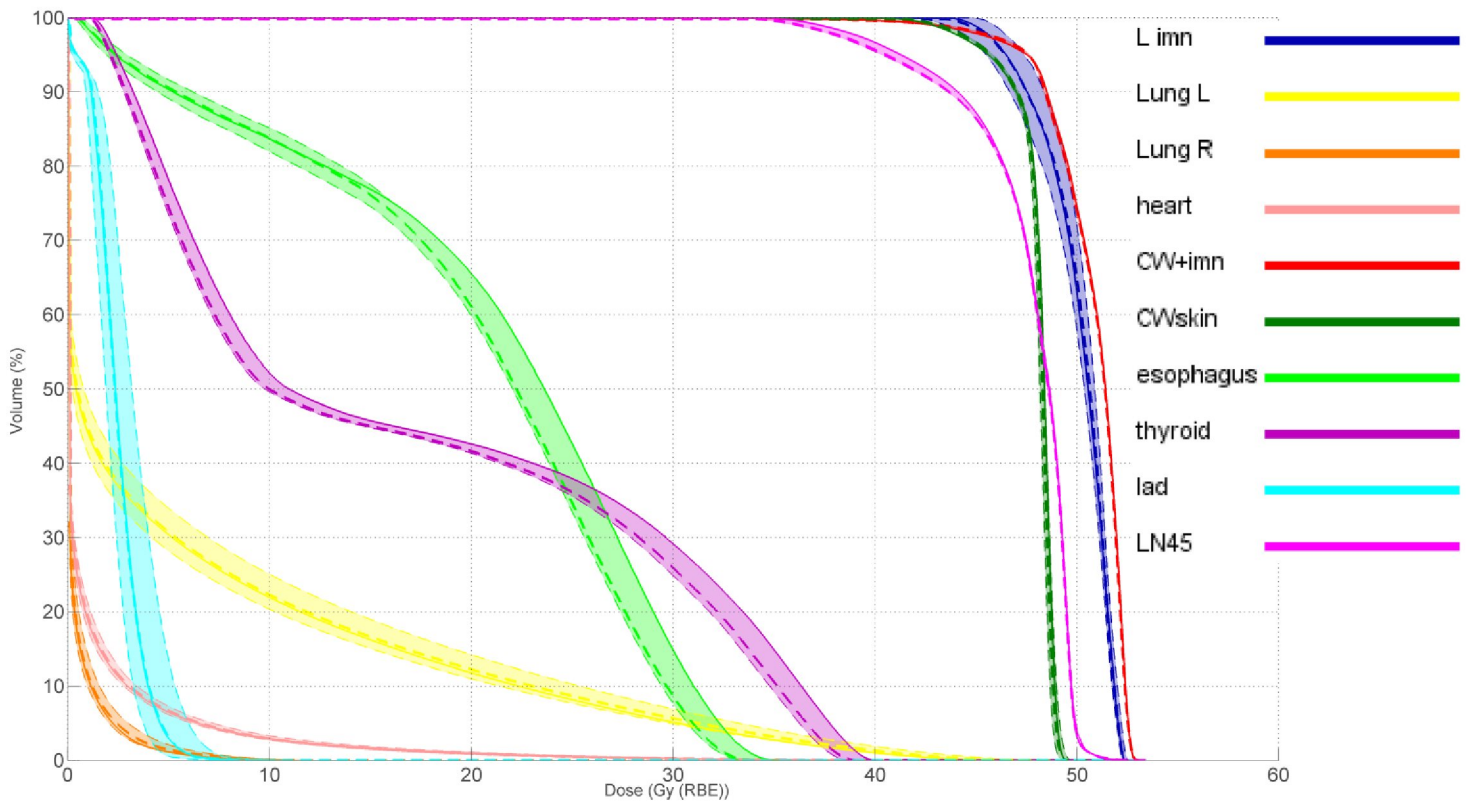


Figure 5: Breathing motion effect onto a static PMRT dose distribution. The solid lines represent the planned dose while the envelopes correspond to the maximal deviations observed from the individual dose recomputations on the 10 phases of the patient 4D scan, and the thick dashed lines is the average dose distribution DVH based on all 10 recomputations.